A Numerical Study on the Ion Production in the INTI International University Plasma Focus Machine using Nitrogen Gas

Arwinder SINGH[1], Teh Thiam OUN[1], Ng Xue YINN[1], Ng Chee AN[1], Wong Jun WEN[1], Saw Sor HEOH[2,3] and Lee SING[1,2,3]

[1]INTI International University, Persiaran Perdana BBN, Putra Nilai, 71800 Nilai, Negeri Sembilan, Malaysia

[2]Nilai International University, No 1, Persiaran Universiti, Putra Nilai, 71800 Nilai, Negeri Sembilan, Malaysia

[3]Institute for Plasma Focus Studies, Chadstone, VIC3148, Australia

([*]Corresponding author's e-mail: arwinders.jigiris@newinti.edu.my)

Abstract

In this paper, a numerical study on the production of ions beam and its energy in nitrogen gas using the Lee model code was carried out using the INTI International University plasma focus machine experimental current waveform results of 480 shots (120 shots at each pressure). It has been found that if the INTI International University plasma focus machine is to be used for material hardening the best results, from the viewpoint of ion beam energy will be obtained at 1 Torr.

Keywords: Numerical experiment, dense plasma focus, Nitrogen gas, Lee model code

Introduction

The dense plasma focus machine is a multiple radiation source of ions, electron, soft and hard x-rays, and neutrons, making it useful for several applications in many different fields such as surface hardening, lithography, radiography, imaging and etc.

In parallel with the laboratory work there has been extensive theoretical, analytical and numerical work on the plasma focus which could be traced back to the original one-fluid formulation of piston-like 'snowplow' model of Rosenbluth [1-5] to 2-D two-fluid MHD models [6] and three-fluid MHD models [7,8]. Kinetic models were extended to fully kinetic simulations [9-12] giving perhaps the most advanced simulations of the plasma focus at the expense of considerable theoretical sophistication and computing resources. On the other hand, simpler methods with varying degrees of utility had been used by others [13-20]. The Lee code [21-24] uses a relatively simple approach and yet is able to achieve the widest range of applications in plasma focus computations.

This paper gives one example of the applications of the Lee code to identify the optimum pressure for nitriding. To understand the performance of a plasma focus machine, the current trace [21], should be analysed because it contains information on the dynamic, electrodynamic, thermodynamic and radiation processes that occur in the various phases of the plasma focus [21-23]. One of the most important procedures therefore is to connect the numerical experiment [24] to the reality of the actual machine by fitting the computed current trace to a measured current trace. [21, 25-31].

Procedure for the numerical study

The machine parameters of the INTI International University plasma focus (denoted in this paper as INTI PF) is as follows. It is a conventional Mather type machine which is part of a network of 3kJ Mather type plasma machine known as the UNU/ICTP PFF (United Nations University/International Centre for Theoretical Physics Plasma Fusion Facility) [32]. It has a capacitance of 30μF, static inductance of 114nH; a circuit resistance of 13 mΩ. This machine has an anode length of 16 cm with a radius of 0.95 cm. The anode is surrounded by cathodes arranged in a circle having a radius of 3.2 cm measured from its center.

In a recent series of experiments over 480 shots, this machine was operated at various pressure of nitrogen gas from 0.5 -2 Torr. The measured current derivative was obtained with a coil and then integrated with respect to time to obtain the current trace. We then configure the Lee's 6 phase model code (version: RADPFV6.1) as the INTI PF by entering the bank parameters, tube parameters and operational parameters.

The computed total current waveform is fitted to the measured waveform by adjusting the model factors f_m, f_c, f_{mr} and f_{cr} one by one, till the computed waveform agrees with the measured waveform [32-36].

The mass swept-up factor f_m accounts for not only the porosity of the current sheet but also for the inclination of the moving current sheet-shock front structure, boundary layer effects, and all other unspecified effects which have effects equivalent to increasing or reducing the amount of mass in the moving structure, during the axial phase. The current factor f_c accounts for the fraction of current effectively flowing in the moving structure (due to all effects such as current shedding at or near the back-wall, and current sheet inclination). This defines the fraction of current effectively driving the structure, during the axial phase.

First, f_m, f_c are adjusted until (see Figure 1) the features (1) computed rising slope of the total current trace and (2) the rounding off of the peak current as well as (3) the peak current itself are in reasonable fit with the measured total current trace.

Then we continue to fit the radial f_{mr} and f_{cr} until features (4) the computed slope and (5) the depth of the dip agree with the measured. The mass swept-up factor f_{mr} takes into account all mechanisms which increase or reduce the amount of mass in the moving slug, during the radial phase. The current factor f_{cr} is the fraction of current effectively flowing in the moving piston forming the back of the slug (due to all effects). This defines the fraction of current effectively driving the radial slug. For the Lee Model 5-phase code the fitting ends here. For the Lee's 6 phase model code the Lee's 5 phase model is extended with a post –pinch phase of anomalous resistance. The good fit of the computed to the measured current waveforms assures that the code has been calibrated to the INTI PF focus machine including known mechanisms such as current sheath porosity and geometry and unknown machine effects such as random edge effects which are not incorporated in the coupled equations of the code but are incorporated through the resultant mass sweeping and effective current fractions.

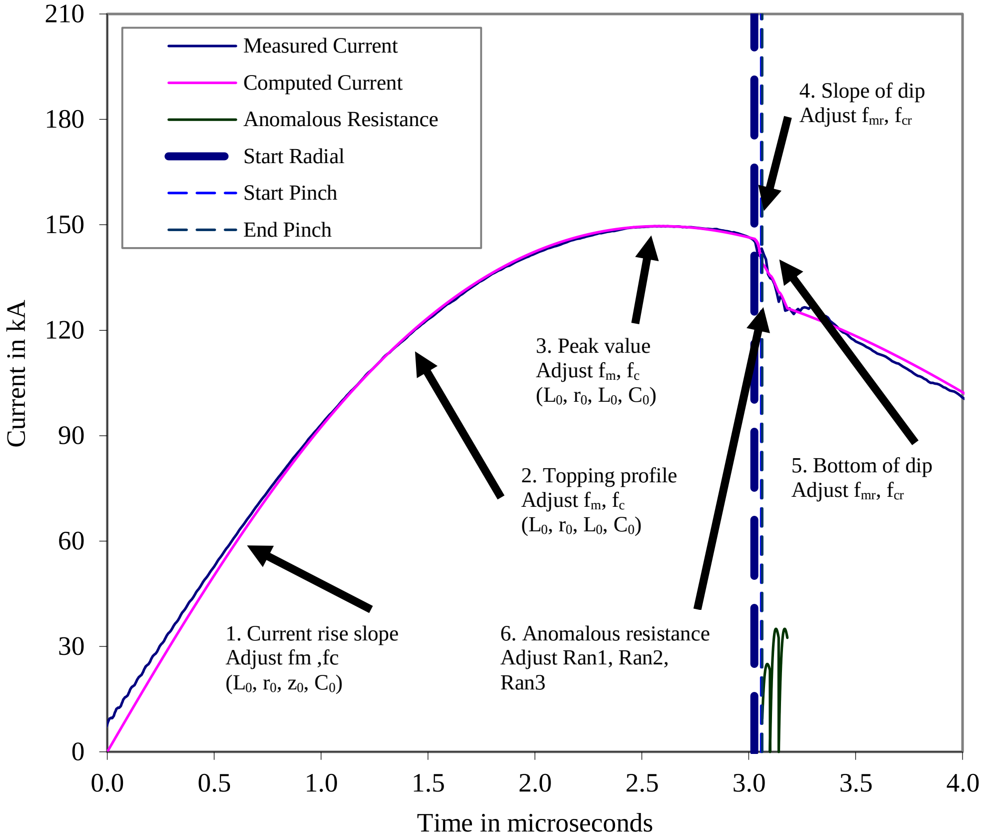

Figure 1 *The 6-point fitting of computed current trace to the measured current trace obtained from shot number 11 of the INTI International University Plasma focus machine operated at 12kV, 0.5 Torr in nitrogen gas. The fitting uses Lee Model 6-phase code.*

The machine, operation and fitted parameters for the fitting above are shown in Table 1.

Table 1 *Machine, operation and fitting parameters for the INTI International University Plasma focus machine used for fitting the numerical experimental current curve to the actual measured current curve. (Nitrogen at 0.5 Torr)*

Capacitance C_0 (μF)	30
Static inductance L_0 (nH)	114
Circuit resistance r_0 (mΩ)	13
Cathode radius ‘b’ (cm)	3.2
Anode radius ‘a’(cm)	0.95
Anode length ‘z_0’(cm)	16
Charging voltage V_0 (kV)	12
Fill gas pressure P_0 (Torr)	0.5
Fill gas(molecular weight)	28
Fill gas(atomic number)	7
Fill gas(molecule(2))	2
Axial phase mass factor, f_m	0.045
Axial phase current factor, f_c	0.53
Radial phase mass factor, f_{mr}	0.07
Radial phase current factor, f_{cr}	0.9

Results and discussion

The computed and measured current traces in Figure 1 show a good fit. The peak current computed is 150 kA and exhibits a radial phase start time of 3.025 μs for pinch duration of 4.463 ns with an all line yield of 3.13μJ (Note: All- line yield consists of the whole range of yields and covers a wide range of wavelengths such as ultra violet, soft X-ray, hard X –ray etc.) The fittings were carried out for all 120 shots for each pressure from 0.5 to 2 Torr and the computed values of the maximum temperature of the pinch, pinch duration, all- line yield, number of ions per shot and beam energy were obtained (Using the fitting parameters which were later input into Lee code model version: RADPFV5.15FIB

From the results, it can be noted that when the Pressure P_0 is increased the axial speed v_a decreases.

Similarly the radial shock speed v_s and the radial magnetic piston speed v_p also decreases. The decrease in the radial shock speed v_s causes a decrease in the temperature of the inward radial shock (the temperature depends on the shock speed to power of 2). This sets the stage for a decreased pinch temperature as pressure P_0 increases (see Figure 2). As these two radial speed decreases, the time required for the radial reflected shock increases and also the pinch duration increases [37,38]. This is shown in Figure 3 from the graph of pinch duration versus pressure.

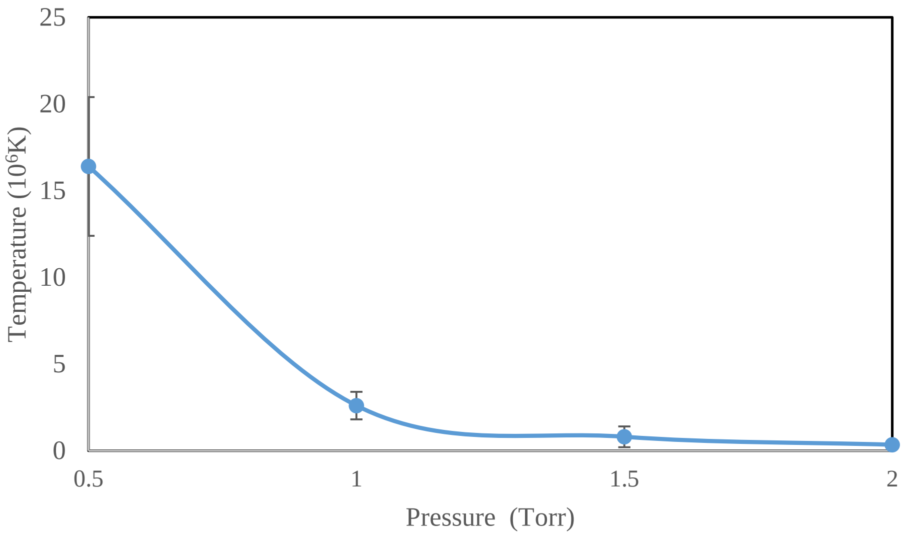

Figure 2 *Temperature of the plasma pinch versus Pressure of the 480 shots taken from measured current curve when they are fitted using the Lee's Model code.*

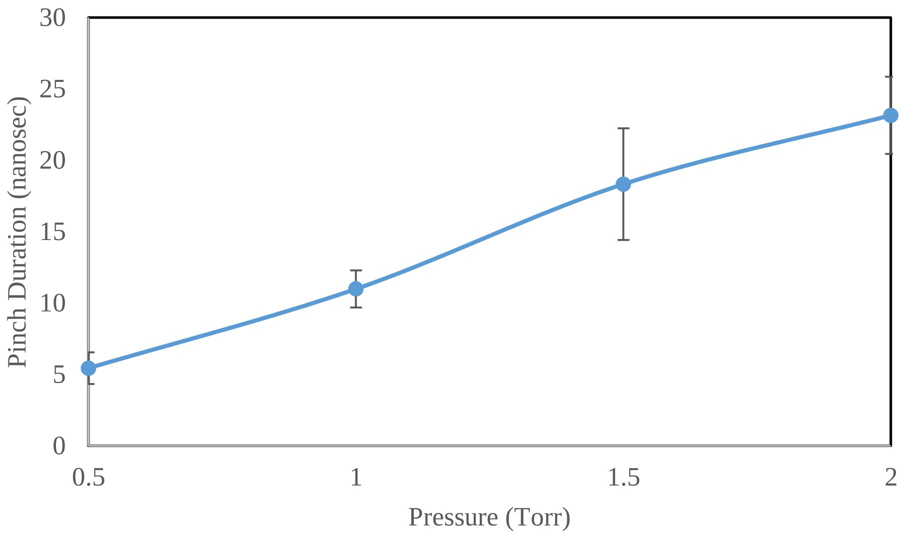

Figure 3 *Pinch duration versus Pressure of the 480 shots taken from measured current curve when they are fitted using the Lee's Model code.*

The ion beam exits the plasma focus pinch along its axis. It is assumed to be a narrow beam (having the same cross-section as the pinch) with little divergence; at least until it overtakes the post-pinch axial shock wave [39-41]. The curve of production of Ions versus pressure in the pinch is shown in Figure 4.

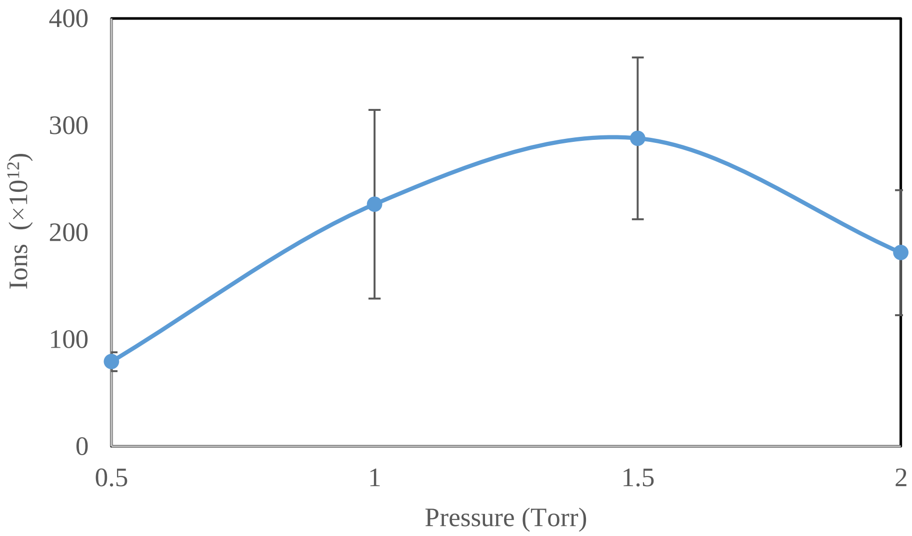

Figure 4 *Number of ions versus Pressure of the 480 shots taken from the Lee code fitted to each measured current curve.*

It should also be noted, that at higher pressure the energy per ion is less than at lower pressure. This can be seen in Figure 5, where the maximum ion beam energy is at 1 Torr whereas the maximum number of ions is at 1.5 Torr as shown in Figure 4.

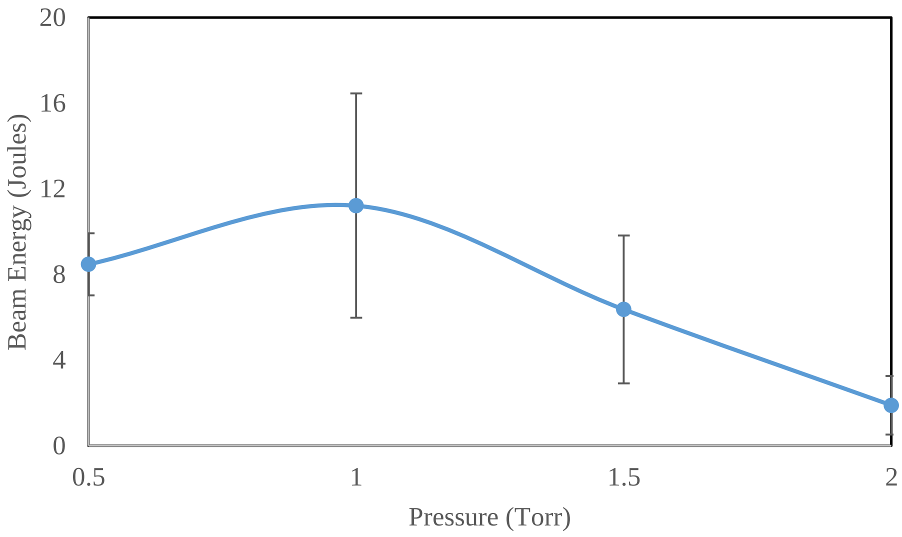

Figure 5 *Beam energy versus Pressure of the 480 shots.*

To study the all- line yield produced in nitrogen for the INTI International University plasma focus machine, it should be noted that the interaction between temperature and pinch density will produce a point where the maximum yield is produce. For INTI International University plasma focus machine this is obtained (by current fitting) at 1 Torr and the probably maximum all- line yield was 0.15 Joules as shown in Figure 6.

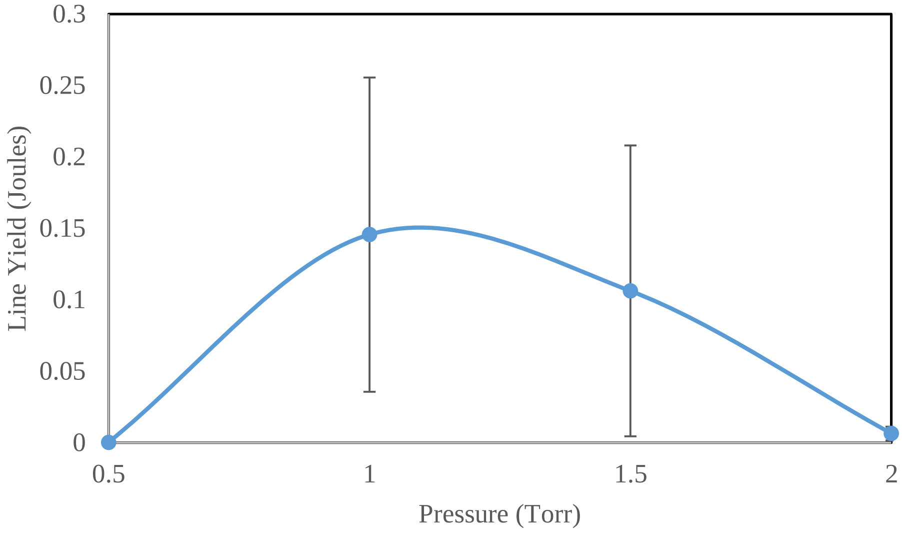

Figure 6 All Line Yield versus Pressure of the 480 shots taken from the Lee code fitted to each measured current curve.

Conclusion

From the Figures above, the Lee code reveals that when INTI International University plasma focus machine is operating, it will produce the maximum ion beam energy at 1 Torr. From this point of view, this may be a good operating pressure for the nitrating of materials as the device produces 16.5 Joules of ion energy at this pressure. This is in the process of being verified by analysis of the corresponding targets which were irradiated during these 480 shots.

The above presentation is an example of how the Lee model code is used to analyse measured current traces to give information of plasma properties and radiation yields.

References

[1] M. Rosenbluth, “Magnetohydrodynamics”, ed. by R. K. M. Landshoff, Stanford University Press, 57, 1957.

[2] F. J. Fishman and H. Petscheck, “Flow model for large radius-ratio magnetic annular shock-tube operation”, Phys. Fluids 11, 632 (1962).

[3] T. D. Butler, I. Henins, F. C. Jahoda, J. Marshall and R. L. Morse, “Coaxial snowplow discharge”, Phys. Fluids 12, 1904 (1969).

[4] K. V. Roberts and D. E. Potter, “Methods of Computational Physics, Academic”, New York, 1970.

[5] A. A. Amsden, “Los Alamos Scientific Laboratory Report”, No.LA-3466 (1966).

[6] D. E. Potter, “Numerical studies of the plasma focus”, Phys. Fluids 14(9), 1911 (1971).

[7] S. V. Bazdenkov and V. V. Vikhrev, Sov. J. Plasma Phys. 1, 250 (1975).

[8] K. Behler and H. Bruhns, “Three-fluid magnetohydrodynamical simulation of plasma focus discharges”, Phys. Fluids 30(12), 3767 (1987).

[9] A. Schmidt, V. Tang and D. Welch, “Fully kinetic simulations of dense plasma focus Z-pinch devices”, Phys. Rev. Lett. 109(20), 205003 (2012).

[10] A. Schmidt, A. Link, D. Welch, J. Ellsworth, S. Falabella and V. Tang, “Comparisons of dense-plasma-focus kinetic simulations with experimental Measurements”, Phys. Rev. E 89 (6), 061101 (2014).

[11] A. Schmidt, A. Link, D. Welch, B.T. Meehan, V. Tang, C. Halvorson, M. May and E.C. Hagen, “Fully kinetic simulations of megajoule-scale dense plasma focus”, Phys. Plasmas 21, 102703 (2014).

[12] A. Schmidt, D. P. Higginson, S. Jiang, A. Link, A. Povilus, J. Sears, N. Benneth, D. V. Rose, D. R. Welch, “Kinetic simulations of dense plasma focus breakdown”. 57th Ann. Mtg. APS Division of Plasma Physics, Savannah, GA, LLNL-ABS-675188. Nov. 16–20, 2015.

[13] J. H. González, A. Clausse, H. Bruzzone and P. C. Florido, “A lumped parameter model of plasma focus”, IEEE Trans. Plasma Sci. 32(3), (1383) 2004.

[14] D. Potter, “The formation of high-density z-pinches” Nucl. Fusion 18(6), 813 (1978).

[15] J. H. González, F. R. Brollo and A. Clausse, “Modeling of the dynamic plasma pinch in plasma focus discharges based in Von Karman approximations”, IEEE Trans. Plasma Sci. 37(11), 2178 (2009).

[16] M. Trunk, “Numerical parameter studies for the dense plasma focus”, Plasma Phys. 17(4), 237 (1975).

[17] V.S. Imshennik, N.V. Fillipov and T. I. Fillipova, “Similarity theory and increased neutron yield in a plasma focus”, Nucl. Fusion 13(6), 929 (1973).

[18] V. Vikhrev and V. D. Korolev, "Neutron generation from Z-pinches", Plasma Phys. Rep. 33(5), 356 (2007).

[19] E. J. Lerner, S. K. Murali and A. Haboub, "Theory and experimental program for the p-B11 fusion with the dense plasma focus", J. Fusion Energ. 30, 367 (2011).

[20] S. K. H. Auluck, "Dense plasma focus: a question in search of answers, a technology in search of applications", Plasma Sci. Appl. Int. J. Mod. Phys. Conf. Ser. 32, 1460315 (2014).

[21] S. Lee and S. H. Saw, "The Plasma Focus- Scaling Properties to Scaling Laws". Joint ICTP-IAEA Workshop on Dense Magnetized Plasma and Plasma Diagnostics, 15 - 26 November 2010.

[22] S. Lee, "Radiation in Plasma", edited by B. Namara. World Scientific, Singapore, Vol II, 978, 1984.

[23] S. Lee, "In Laser and Plasma Technology", edited by S. Lee, B.C. Tan, C.S.Wong and A.C.Chew. World Scientific, Singapore, 37, 64 and 387, 1985.

[24] S. Lee, Radiative Dense Plasma Focus Computation Package: RADPF, 2014
http://www.plasmafocus.net
http://www.plasmafocus.net/IPFS/modelpackage/File1RADPF.htm
http://www.plasmafocus.net/IPFS/modelpackage/File2Theory.pdf
http://www.plasmafocus.net/IPFS/modelpackage/UPF.htm;

[25] S. Lee and S. H. Saw, "Neutron scaling laws from numerical experiments". J. Fusion Energy 27, 292 (2008).

[26] S. Lee, "Neutron Yield saturation in Plasma –focus. A fundamental cause", Appl. Phys. Lett. 95 (15), 151503 (2009).

[27] S. Lee, S. H. Saw, L. Soto, S. V. Springham and S. P. Moo, "Numerical experiments on plasma focus neutron yield versus pressure compared with laboratory experiments", Plasma Phys. Control Fusion 51, 075006 (2009).

[28] S. H. Saw and S Lee, "Scaling laws for plasma focus machines from numerical experiments", Energ. Power Eng. 2010, 65 (2010).

[29] S. Lee and S. H. Saw, "Numerical experiments providing new insights into plasma focus fusion devices", Energies 3(4), 711 (2010).

[30] S. H. Saw and S. Lee, "Scaling the plasma focus for fusion energy considerations", Int. J. Energy Res 35, 81 (2011).

[31] S. Lee and S. H. Saw, "The plasma focus: Trending into the future, Int. J. Energy. Res. 36(15), 1366 (2012).

[32] S. Lee, T. Y. Tou, S. P. Moo, M. A. Eissa, A. V. Gholap, K. H. Kwek, S. Mulyodrono, A. J. Smith, Suryadi, W. Usada and M. Zakaullah, "A simple facility for the teaching of plasma dynamics and plasma nuclear fusion", Am. J. Phys. 56, 66 (1998).

[33] T. Y. Tou, S. Lee and K. H. Kwek, "Nonperturbing plasma-focus measurements in the run-down phase", IEEE Trans. Plasma Sci., 17, 311 (1989).

[34] S. P. Chow, S. Lee and B. C. Tan, “Current sheath studies in a co-axial plasma focus gun”, J. Plasma Phys., 8, 1 (1972).

[35] Sh. Al-Hawat, M. Akel , S. Lee and S. H. Saw, “Model parameters vs gas pressure in two different plasma focus devices operated in argon and neon”, J. Fusion Energ. 31, 13 (2012).

[36] S. Lee, S. H. Saw, H. Hegazy, Jalil Ali, V. Damideh, N. Fatis, H. Kariri, A. Khubrani and A. Mahasi, “Some generalised characteristics of the electro dynamics of the plasma focus in its axial phase-illustrated by an application to independently determine the drive current fraction and the mass swept-up fraction”, J Fusion Energ. 33, 235 (2014).

[37] S. Lee and A. Serban. “Dimensions and lifetime of the plasma focus pinch”, IEEE Trans. Plasma Sci. 23(3), 1101 (1996).

[38] S. Lee, “Plasma focus radiative model-review of the Lee model code”, J. Fusion Energ. 33, 319 (2014).

[39] M. Akel, S. A. Salo, S. H. Saw and S. Lee. “Characterization of oxygen beams emitted from plasma focus”, Vacuum 110, 54 (2014).

[40] M. Akel, S. A. Salo, S. H. Saw and S. Lee. “Ion beam features produced by two plasma focus machines operated with different gases”, IEEE Trans. Plasma Sci. 42(9), 2202 (2014).

[41] M. Akel, S. A. Salo, S. H. Saw and S. Lee. “Properties of ion beams generated by nitrogen plasma focus”, J. Fusion Energy 33(2), 189 (2014).

Effect of Coaxial Dielectric Barrier Discharge Reactor Configuration on CO_2 Decomposition

Yutthana TIRAWANICHAKUL[1*] and Nikom PHUENGKUM[2]

[2]ThEP Center, CHE, 328 Si Ayutthaya Rd., Bangkok 10400, Thailand
[1]Membrane Science and Technology Research Center, Faculty of Science, Prince of Songkla University, Hatyai, 90110 Songkhla, Thailand
[1,2]Plasma and Energy Technology Research Laboratory, Department of Physics, Faculty of Science, Prince of Songkla University, Hatyai, 90110 Songkhla, Thailand

([*]Corresponding author's e-mail: yutthana.t@psu.ac.th)

Abstract

For four decades the dielectric barrier discharges (DBDs) has been well-known non-thermal plasma discharges for various applications in science and environment concern such as ozone synthesis, gas decomposition and conversion, air pollution control, excimer laser, material and film surface modifications etc. Thus, the main objective of this present work was to study effect of reactor electrodes configuration on CO_2 decomposition. The quartz coaxial tube was designed as DBD plasma reactor for decomposition of gas. The outer electrode and inner electrode was made of thin flat copper sheet and stainless-steel rod, respectively. The electrical discharge gap between both of electrodes was fixed at 0.5 mm. The argon plasma discharge was generated by a high AC voltage (0-8 kV) with fixed frequency of 7.8 kHz. The inlet mixed gas ratio, discharge gap, applied voltage, outer electrode length, step of gas discharges and inlet gas flow rate was varied in each operating condition. The results showed that percentages of CO_2 conversion relatively decreased with increase of mixing ratio of CO_2:Ar and inlet mixing gas flow rate. In controversy, percentage increase of CO_2 conversion significantly related to high voltage supply. Furthermore, the high percentage of CO_2 conversion (47.2%) has been obtained at 1.3 mm electrical discharge gap.

Keywords: Gas conversions; DBD reactor; Pollution control; Greenhouse gases (GHG)

Introduction

CO_2 is a part of greenhouse gases and has been attracting to the global warming on the earth. It can be more emitted from the transportations, burning and the use of all fossil fuels. The chemical bond of CO_2 is very strong and cannot be dissociate in using of chemical reaction. To dissociate the OC=O double bond, the high temperature has to use at least 1,500°C for thermolysis process and high pressure has been employed to break CO_2. However, this dissociation results are quite low performance comparing to its investment. Even there are many methods to convert CO_2 such as photo-catalytic and photochemical processes, Biochemical processes and Physical processes but it seems to be insufficient process to huge amount of CO_2 conversion in the short period. The most effective process should be easy and encourage us to work on conversion of CO_2. The non-thermal plasma processes have been studied and adopted to avoid those low perform incidences such as glow discharge, corona discharge, dielectric barrier discharge (DBD), radio frequency (RF) discharge and microwave discharge etc. [1-9]. In addition, Indarto *et al.* [1] have been reported the review article about greenhouse gas and toxic gas decompositions through the plasma technologies. In summary, they suggested that the advantage process should be the combined or new alternative process and methods. DBD plasmas had been promoted for a long time for surface modifications, gas treatment, synthesis, etc. The characteristic of DBDs system can initiated plasma and gas reactions using low energy consumption and low temperature at near atmospheric pressure. Even this system is low temperature plasma discharge but electron particles still have high energy enough (ranging of 1-100 eV) to dissociate and breakdown the chemical bond of gas molecules directly [1, 3, 15-19] and modify surface of poly styrene (PS), poly methyl methacrylate (PMMA) and 1:1 mixture of PS:PMMA films in atmosphere [20-23]. The CO_2 conversion using DBD reactor was operated under various conditions such as gas flow rate, gas temperature, power frequency and power input [24]. In addition, some previous work suggested and represented that noble gas containing in gas feeding or placing a solid catalyst in plasma zone can raise the rate of the gas conversion and product yield [1, 4, 6, 12] and it also produced carbon nanotube on the catalyst surface. Furthermore, Tao *et al.* [25] has reported the reviewed article for the opportunity of CH_4-CO_2 reforming in different methods and they suggested that to improve high performance in plasma process for reforming gas there were three factors which were comprised of reactor configuration, electron density and plasma temperature. Recently, Weizong *et al.* [26] reported a gliding arc plasma could convert CO_2 into CO and O_2. a self-consistent two-dimensional (2D) gliding arc model was developed. Their calculated values of the electron number density in the plasma showed reasonable agreement with the experiments.

Thus the main objective of this research was to study effect of physical parameters on CO_2 decomposition via AC high voltage with high frequency applied. The experiments were carried on under the conditions of 4 different mixing gas ratio of carbon dioxide and argon, various applied voltage between 4 and 8 kV, 3 discharge gap interval and 2 electrode configurations. And finally, the suitable operating condition and effect of those parameter on CO_2 decomposition were discussed and presented.

Materials and methods

Theory

The reaction of plasma chemistry for CO_2 decomposition can be shown in Eq.(1) and Eq. (2), after the process of CO_2 decomposition, this CO_2 is converted into CO and O_2 [10-12]. Eq. (1) and Eq. (2) had confirmed that CO and O_2 are the main product, where ΔH is the enthalpy of the reaction. However, O_2 can formed by the recombination of O radicals, and similarly CO_2 also has reformed by the recombination of CO with O radicals and C with O_2 [1, 13]. CO gas product was utilized for hydrocarbon fuel synthesis (e.g. methanol, ethanol and acetic acid synthesis) and for the mineral and metal industries (e.g. smelting and refining processing).

$$\mathrm{CO_2 \rightarrow CO + \tfrac{1}{2}O_2, \Delta H = 2.9\ eV/mol} \tag{1}$$

$$\mathrm{CO_2 \rightarrow CO + O, \Delta H = 5.5\ eV/mol} \tag{2}$$

On the one hand, it can be considered in the unit of Joule [14].by following equation below

$$\mathrm{CO_2 \rightarrow CO + O, \Delta H = 529.8\ kJ/mol} \tag{3}$$

Due to low energy treatment for these chemical reaction, the way to approach CO_2 conversion process by non-thermal plasma discharge can be performed and the high CO_2 conversion in this plasma technique will be studied in this work by following experimental set up below.

Experimental set up

The experimental set up was carried out as shown in Fig. 1 which the system consisted of sample feed tanks of purified CO_2 and Ar gas and their accessories (gas regulator, butterfly valve, flow meter, mixer unit, needle valve), coaxial DBD reactor, bubble flow meter, high voltage power supply. For measurement, high voltage (HV) probe (Tektronix, P6015A) which was crossed between high voltage line and ground the resistor and connected to digitized storage oscilloscope (Tektronix, TDS3014B), was used for detection HV input of DBD reactor while the charge transfer can be measured from voltage across C_m by using voltage probe. These parameters of applied voltage and charge transfer were utilized to calculate the power consumption by Q-U Lissajous plotting [26]. The mixing gas before and after treatment by quartz tube DBD in each operating condition was evaluated by gas analyzer (Geotech, Biogas Check). A quartz tube 1 mm of thickness with inner diameter 12 mm was provided as DBD plasma reactor. Both flanges closing reactor tube was made of Teflon insulator and used for stainless steel inner electrode support to protection HV shock and outer electrode was made of Aluminum flat sheet wrapping around the tube while stainless steel rod is placed at center of the quartz tube and acted as inner electrode.

Effect of discharge gap and two outer electrodes, CO_2 concentration, outer electrode length and applied voltage on CO_2 decomposition were evaluated and presented in the next section.

To evaluate the performance of the DBD system for CO_2 decomposition, the percentage of CO_2 conversion (χ_{conv}), O_2 selectivity (O_{2s}), power consumption and conversion efficiency were determined by following Eq. 4 and 5, respectively. The following equation for calculating of CO_2 conversion and O_2 selectivity can be written as below [15, 24].

$$\chi_{\mathrm{conv}}\ (\%) = \frac{\mathrm{CO_2\ converted\ (mol)}}{\mathrm{CO_2\ input\ (mol)}} \times 100 \tag{4}$$

$$\mathrm{O_{2s}}\ (\%) = \frac{\mathrm{O_2\ product\ (mol)}}{\mathrm{CO_2\ converted\ (mol)}} \times 100 \tag{5}$$

Additionally, the power consumption (P_E) can be determined by integrating energy consumption during operating period as illustrated in Eq.6 while the conversion efficiency (η_{conv}) from Eq. 7 has been adopted from the previous works [2, 26] as shown below.

$$\mathrm{P_E\ (W)} = \mathrm{f} \cdot \mathrm{C_m} \int_0^{\mathrm{T}} \mathrm{U_t du_c} \tag{6}$$

$$\eta_{\mathrm{conv}}(\%/\mathrm{W}) = \frac{\mathrm{CO_2\ conversion\ (\%)}}{\mathrm{P_E\ (W)}} \tag{7}$$

where f = fixed frequency of power source used, kHz

C_m = certain measuring capacitor which was used for determining voltage drop by voltage probe

U_t = applied voltage, V

u_c = voltage across certain measuring capacitor, V

In this experiment the frequency of power source was fixed at 7.8 kHz and the certain measuring capacitor was fixed at 10 nF.

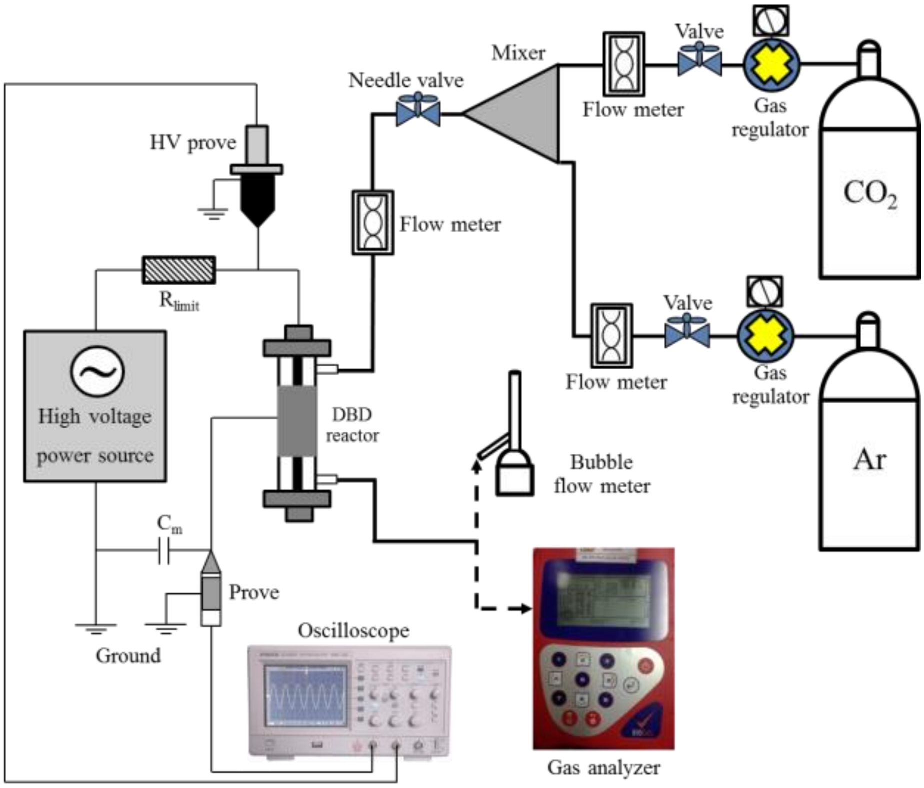

Figure 1. *Experimental set up of CO_2 conversion process by plasma dielectric barrier discharges*

Results and discussion

Characteristic of Plasma in DBD system

To verify the DBD system on its configuration before doing each experiment, the DBD system was constructed following on the Fig. 1. However, studying effect of electrode shape configuration, the two outer electrode shapes configuration were proposed in this research and tested at the same operating conditions (power supply of 8 kV 7.8 kHz). Fig.2 illustrated corona discharge pattern of the two different outer electrode shape configuration which was installed into single part outer electrode shape (Fig. 2A) and double parts outer electrodes shape (Fig. 2B), respectively. From the figures its non-thermal plasma discharges of the two electrode shapes configuration was similar pattern with purple color corona discharges. This is because the gas inlet flowing pass through DBD gap was ambient air which is mostly consists of nitrogen gas (atmospheric pressure) [8, 12].

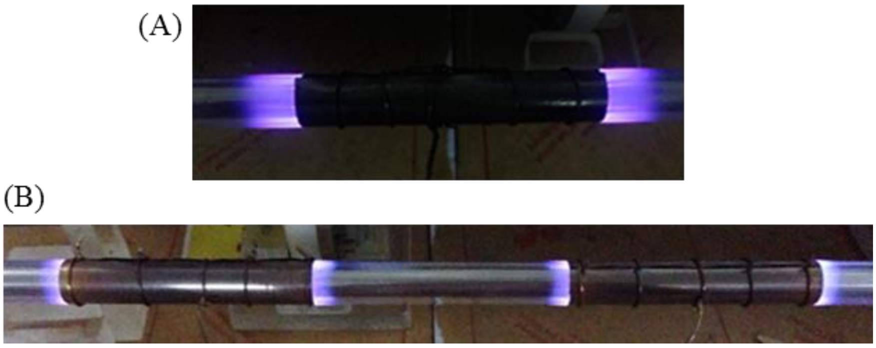

Figure 2. *Corona discharge of DBD plasma reactor with single part outer electrode shape (A) and double parts outer electrodes shape (B) with distance apart of 8 cm*

The consumed energy in the reactor was determined by voltage–charge curve (V–Q Lissajous figure). In the previous experiment [15], the consumed energies obtained with V–Q Lissajous figure were checked by comparing with the values calculated from the time integral of the product of the applied voltage and the current [16]

Effect of CO_2 concentration

To study effect of CO_2 concentration on CO_2 conversion and O_2 selectivity, the purified CO_2 gas and Ar gas were feed in to mixing tube using ranging between 60% and 90% by volume. The accurate mixing gas flow rate was controlled by needle valve and fixed at 50 ml/min while discharge gap of 1.30 mm width, and outer electrode length of 8 cm and applied voltage across the electrodes was about of 8 kV. By calculation with Eq.(4) and Eq.(5), plotting graph between CO_2 conversion and concentration of CO_2 was illustrated in Fig.3. The experimental results showed that the increase of CO_2 concentration causes CO_2 conversion decreased. On the other hand, O_2 selectivity which was the gas product has higher increased at 80% of CO_2 concentration. The low mixing ratio of CO_2 concentration replied that a high amount of Ar plasma discharges increased the collision of gas reaction in discharge zone between electrodes. This is because Ar after breakdown (as plasma state) provides more electrons and ions. This result is corresponded to the previous research works [1, 11-12, 21].

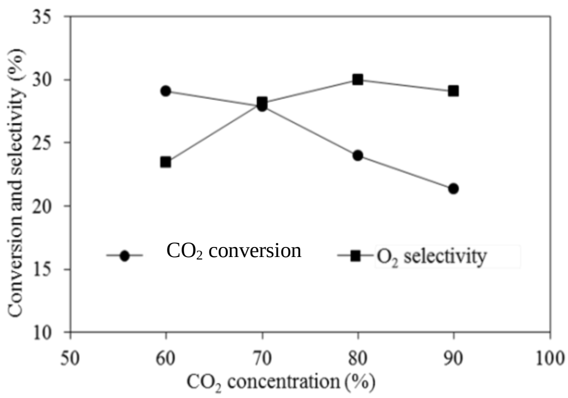

Figure 3*. Effect of CO_2 concentration on CO_2 conversion and O_2 selectivity*

Effect of electrode configuration and applied voltage

To study effect of electrode configuration on CO_2 conversion. the experimental condition was carried on certain conditions of 50 ml/min of gas flow rate and percentages of mixing ratio of CO_2 and Ar at 60:40. Two types of DBD plasma reactor with single part outer electrode shape and double parts outer electrodes shape outer electrodes configuration were shown in Fig. 2(a) and 2(B), respectively. Moreover, the Ar plasma discharge between coaxial discharge gap between inner and outer electrodes were chosen at 1.3 mm and 2.8 mm of spacing gap (Fig. 5), respectively. Then the experimental results of CO_2 conversion and O_2 selectivity were plotted along with applied voltage cross electrodes and 2 different discharge spacing gap of 1.3 and 2.8 mm. as illustrated on Fig. 4 and Fig.5, respectively. The results showed that the percentage of CO_2 conversion (Bold line in Fig.4 and Fig.5) and percentage of O_2 selectivity (dot line in Fig.4 and Fig.5) were relatively affected by the applied voltage and outer electrode length whilst the discharge spacing gap gave a little effect to the percentage of CO_2 conversion and percentage of O_2 selectivity comparing to the parameters mentioned above. In addition, the Ar plasma discharge occurring at discharge gap for 8 cm and 10 cm of outer electrode lengths tended to increase percentage of CO_2 conversion because the longer outer electrode length had a long period of CO_2 dissociation. The conclusion was stated that the applied voltage across electrodes and outer electrode length significantly affected to increasing of percentage of CO_2 but low affected to percentage of O_2 selectivity.

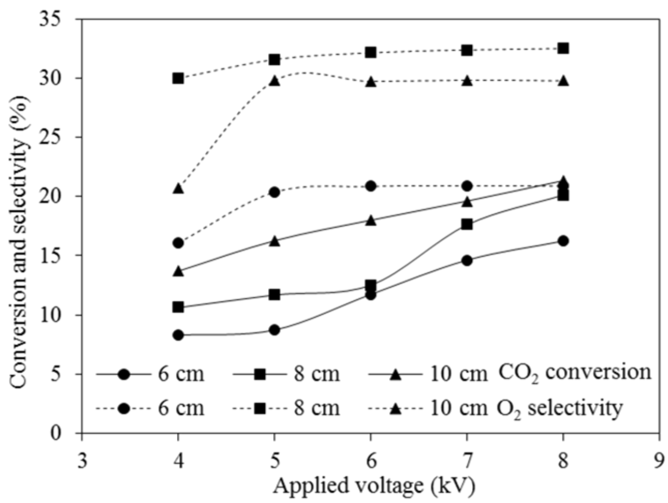

Figure 4 *Effect of outer electrode length and applied voltage on CO_2 conversion and O_2 selectivity at 1.3 mm of discharge gap*

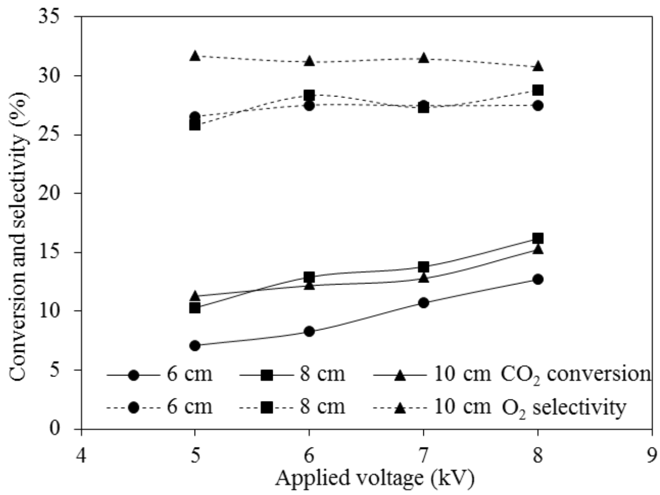

Figure 5 *Effect of outer electrode length and applied voltage on CO_2 conversion and O_2 selectivity at 2.8 mm of discharge gap*

To clarify effect of discharges spacing gap and outer electrode shape on percentage of CO_2 conversion and percentage of O_2 selectivity, the experiments were run and illustrated on Fig.6 and Fig.7, respectively. The discharge spacing gap was varied between 0.4 mm and 2.8 mm and outer electrode length of 8 cm, gas flow rate of 50 ml/min and high percentage mixing ratio of CO_2:Ar at 80:20. Fig.6 illustrated relationship between percentage of CO_2 conversion and applied voltage across electrodes at 3 different discharge gaps. The experimental results showed that the percentage of CO_2 conversion is the highest value at discharge spacing gap of 1.3 mm especially on the double outer electrodes shape with 1.3 mm of discharge gap (1.3 mm, 2OE on Fig.6)

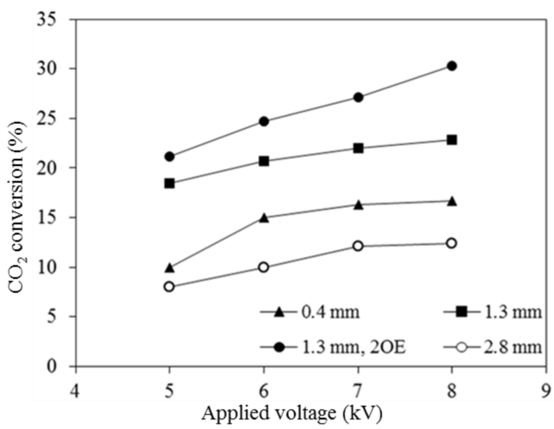

***Figure 6**. Effect of discharge gap and two outer electrodes (2 OE) on CO_2 conversion*

Due to determine percentage of O_2 selectivity, the result was illustrated on Fig. 7 which could be stated that the percentage of O_2 selectivity using discharge gap of 1.3 mm width slight decreased when the applied voltage increase.

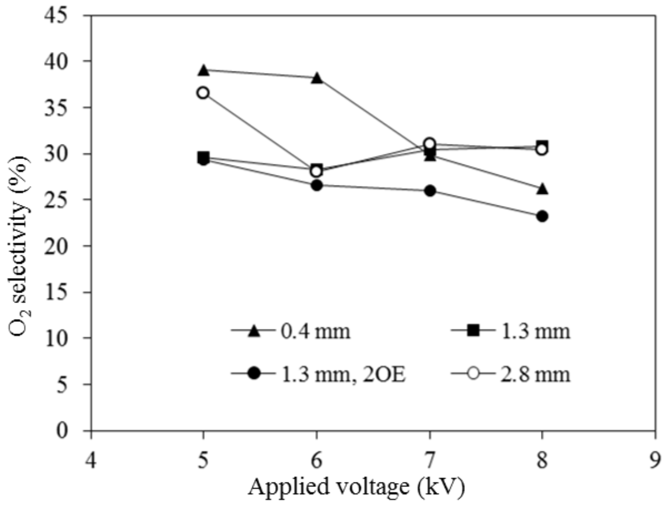

Figure 7. *Effect of discharge gap and two outer electrodes (2 OE) on O_2 selectivity*

Power consumption and conversion efficiency

From Eq.(6) and Eq.(7), the energy consumption and conversion efficiency can be determined and showed in Fig.8-10. The percentage of CO_2 conversion increase with increase of applied voltage across both electrodes and increase of mixing gas flow rate. Fig.8 stated that the energy consumption of plasma discharges system increased with increase of applied. On the other hand, the percentage of conversion efficiency decreased when an applied voltage increased. However, the result has indicated that the high efficiency of CO_2 conversion can be achieved at 1.3 mm of discharge gap of single outer electrode and 1.3 mm of discharge gap with double outer electrodes as shown in Fig.9 and Fig.10.

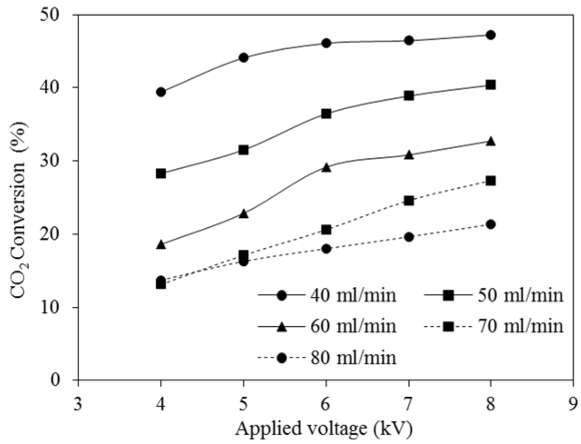

Figure 8 *Effect of gas flow rate and applied voltage on CO_2 conversion and O_2 selectivity*

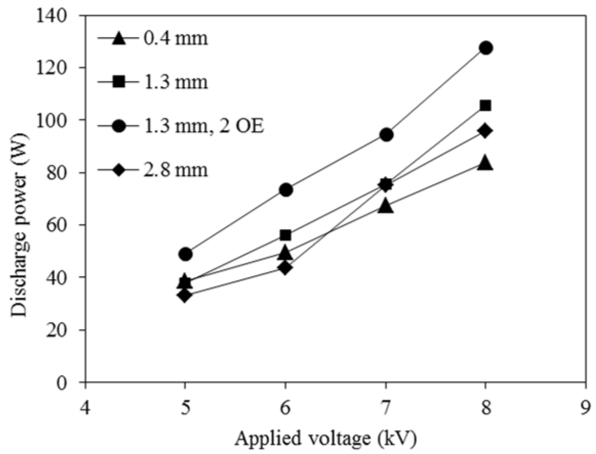

Figure 9 *Discharge power versus applied voltage for each discharge gap*

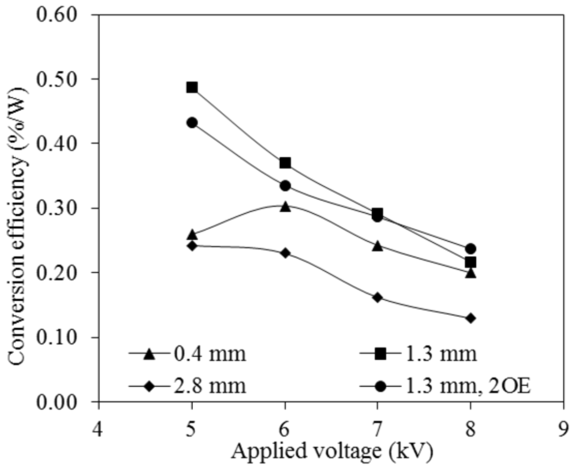

Figure 10 *Conversion efficiency versus applied voltage for each discharge gap*

Conclusion

In summary, this research work had obviously exhibited that the use of the longer outer electrode and double outer electrodes configuration with narrow discharge gap had high performance comparing to the other operating condition. It replies that plasma dielectric barrier discharge system can be used for enhancing CO2 conversion. In similarity, the increase of applied voltage across electrodes and the lower flow rate of mixing gas can also improvable technique for enhancing percentage of CO_2 conversion.

Acknowledgements

The authors would like to sincere thank Thailand Center of Excellence in Physics (ThEP) and Graduate school, Prince of Songkla University, including a research fund and a PhD scholarship. Authors also thank to Membrane Science and Technology Research Center, Department of Physics, Faculty of Science, Prince of Songkla University for their support on experiment area and equipment.

References

[1] A. Indarto, et al., "Decomposition of greenhouse gases by plasma", Environ. Chem. Lett. 6(4), 215 (2008).

[2] S. Wang, et al., "Enhancement of CO_2 conversion rate and conversion efficiency by homogeneous discharges", Plasma Chem. Plasma Proc. 32, 979 (2012).

[3] D. Lee, et al., "Mapping plasma chemistry in hydrocarbon fuel processing processes", Plasma Chem. Plasma Proc., 32, 1 (2012).

[4] A. Indarto, et al., "Gliding arc plasma processing of CO_2 conversion", J. Hazard. Mater. 146(1–2), 309 (2007).

[5] M. Babaie, et al., "Performance evaluation of non-thermal plasma on particulate matter, ozone and CO_2 correlation for diesel exhaust emission reduction", Chem. Eng. J. 276, 240 (2015).

[6] Y. Wen, and X. Jiang, "Decomposition of CO_2 using pulsed corona discharges combined with catalyst", Plasma Chem. Plasma Proc. 21(4), 665 (2001).

[7] K. Yoshida, B.S. Rajanikanth, and M. Okubo, "NO_x reduction and desorption studies under electric discharge plasma using a simulated gas mixture: A case study on the effect of corona electrodes", Plasma Sci. Technol. 11(3), 327 (2009).

[8] L. Xiang, T. Xumei, and Y. Yongxiang, "An atmospheric-pressure glow-discharge plasma jet and its application", IEEE Trans. Plasma Sci. 37(6), 759 (2009).

[9] C. M. Du, J. H. Yan, and B. Cheron, "Decomposition of toluene in a gliding arc discharge plasma reactor", Plasma Sources Sci. Technol. 16, 1 (2007).

[10] A. Fridman, ed. "Plasma Chemistry", Cambridge University Press: New York. 978, 2008.

[11] L. Spencer, and A. Gallimore, "Efficiency of CO_2 dissociation in a radio-frequency discharge", Plasma Chem. Plasma Proc. 31(1), 79 (2011).

[12] D. Mei, et al., "Plasma-photocatalytic conversion of CO_2 at low temperatures: Understanding the synergistic effect of plasma-catalysis", Appl. Catalysis B: Environ. 2015.

[13] Q. Yu, et al., "Characteristics of the decomposition of CO_2 in a dielectric packed-bed plasma reactor", Plasma Chem. Plasma Proc. 32(1), 153 (2012).

[14] G. Zheng, et al., "The mutual conversion of CO_2 and CO in dielectric barrier discharge (DBD)" Plasma Chem. Plasma Proc. 23(1), 59 (2003).

[15] M. Danhua, et al., "Plasma-assisted conversion of CO_2 in a dielectric barrier discharge reactor: Understanding the effect of packing materials", Plasma Sources Sci. Technol. 24(1), 015011 (2015).

[16] C. Tendero, et al., "Atmospheric pressure plasmas: A review", Spectrochim. Acta Part B: Atom. Spec. 61(1), 2(2006).

[17] E. Wagenaars, R. Brandenburg, W. J. M. Brok, M. D. Bowden and H.-E. Wagner, Experimental and modelling investigations of a dielectric barrier discharge in low-pressure argon", J. Phys. D: Appl. Phys. 39(4), 700 (2006).

[18] H.E. Wagner, et al., The barrier discharge: Basic properties and applications to surface treatment", Vacuum 71(3), 417 (2003).

[19] U. Kogelschatz, "Dielectric-barrier discharges: Their history, discharge physics, and industrial applications", Plasma Chem. Plasma Proc. 23(1), 1 (2003).

[20] A. M. G. Borges, et al., "Polymer films with surfaces unmodified and modified by non-thermal plasma as new substrates for cell adhesion", Mater. Sci. Eng. C 33(3), 1315 (2013).

[21] N. De Geyter, R. Morent, and C. Leys, "Surface characterization of plasma-modified polyethylene by contact angle experiments and ATR-FTIR spectroscopy", Surf. Interf. Anal. 40(3-4), 608 (2008).

[22] F. Busnel, et al., "Modification of sugar maple (Acer saccharum) and black spruce (Picea mariana) wood surfaces in a dielectric barrier discharge (DBD) at atmospheric pressure", J. Adhesion Sci. Technol. 24(8-10), 1401 (2010).

[23] M. Šimor, et al., "The influence of surface DBD plasma treatment on the adhesion of coatings to high-tech textiles", J. Adhesion Sci. Technol. 24(1), 77 (2010).

[24] S. Paulussen, et al., "Conversion of carbon dioxide to value-added chemicals in atmospheric pressure dielectric barrier discharges", Plasma Sources Sci. Technol. 19(3), 034015 (2015).

[25] X. Tao, et al., "CH_4–CO_2 reforming by plasma: Challenges and opportunities", Prog. Energ. Combust. Sci. 37(2), 113 (2013).

[26] N. Phuengkum, and Y. Tirawanichakul, "Physics applications: IV characteristics of CO_2 and O_2 dielectric barrier discharges", IEEE Colloquium on Humanities, Science and Engineering, 2011.

Odor Eliminator Using Pulse Cool-Corona Electric Field Net

Siseerot KETKAEW*

Faculty of Engineering, Ramkhamhaeng University, Bangkapi, Bangkok 10240, Thailand

(*Corresponding author's e-mail: siseerot@hotmail.com)

Abstract

This research presented the odor eliminator using pulse cool-corona electric field net on principle of (plasma) corona discharge and electric field intensity changing technique. The power supply based on flyback converter comprises of a pulse generator using NO. IC#SG3526 for the electric field intensity adjustment at 5 kV/cm, 10 kV/cm, and 15 kV/cm under switching frequency adjustment at 20 kHz, 30 kHz and 40 kHz, respectively, and high frequency pulse transformer was used as a ground isolator and signal expanding for Power MOSFET#IRFP460 driving to control high voltage switching transformer to generate 1 kV, 2 kV and 3 kV by using cell electrode (electric field net) for generate ozone gas. The experimental results are switching frequency increasing of high voltage at 1 kV equal to 20 kHz, 2 kV equal to 30 kHz, and 3 kV equal to 40 kHz which the testing of ozone gas quantity measuring will observation at electric field intensity equal 5 kV/cm enables generate ozone gas 3.96 ppm, 10 kV/cm enables generate ozone gas 4.43 ppm and 15 kV/cm enables generate ozone gas 5.83 ppm. By ozone gas 5.83 ppm can be used to get rid of VOCs gas which fruticosa is a foul odor, as well. Odor eliminator through the international standards of Electromagnetic Compatibility, EMC [CISPR 14-1 (CE, Click, PE), IEC 61000-3-2 (HE), IEC 61000-3-3 (VF), CISPR 14-2 (CI, ESD, EFT, Surge, Vdip, PFM) and Tested analyze the Power Consumption are completed. Testing at the test room of electrical and electronic products testing center (PTEC), NSTDA, Thailand. Therefore this research was funded activities to promote and support research of the National Research Council of Thailand (NRCT) 2016 and can be developed into commercial innovations in the future.

Keywords: odor eliminator, cool-corona, electric field, corona discharge, pulse

Introduction

Nowadays, ozone gas is brought to use many ways in everyday life. In practice, ozone gas has both good and bad points – up to what to use for everyday life. This is the result to find a method and control the ozone gas quantity in order to obtain a good result for the society as much as possible. The way is to construct the ozone gas generator with high voltage inverter. The occurred ozone is from the oxygen's molecules dispersion. Oxygen was brought through the producing steps of a dc high voltage, which is from a high voltage switching power supply by using IC#SG3526. This IC will generate the Pulse Width Modulation (PWM) to use for controlling the flyback inverter, which has a Power MOSFET as a switching device. Power MOSFET is the voltage controlled device and need very low input current. Furthermore, there is a high speed switching nano seconds of the unit of very low timing that can provide a high frequency switching. This is the good point to apply with high frequency job. In this case, the high frequency will be applied for a high frequency transformer to get a high voltage square wave about 20,000 volts. Then, high voltage is supplied to the ozone tube. The energy from electric field is the factor that effects to the efficiency of producing ozone gas directly. The type of ozone tubes has to be supported for providing the corona effect to burst oxygen's molecules. This takes place a kind of ozone gas from the equation, $O_2 + O = O_3$. Under high voltage condition, air can be breakdown. In addition, The deteriorated air can make the molecule's structure changing to be ozone gas. However, the endurable limit of voltage effects to the break down of air, causing the generated ozone to vanish during heat from breaking down. Thus, to generate ozone gas, power and frequency have to be controlled. The energy consume for generating ozone gas is defined from the chemical energy that is between 493.2 kJ/mol – 682.8 kJ/mol [1]. This energy can be transformed to other unit. The necessary energy areas are from 5.58 kWh/m^3 – 7.73 kWh/m^3.

Since there is approximately 21% oxygen in the air, the necessary energy for generating ozone gas is between 1.172 kWh/m^3 and 1.62 kWh/m^3 that is enough for occurring ozone gas in the gap [1].

Therefore, this present there are a lot of toxic air pollution caused by dust, odor, different kinds of smoke and etc. They always make human lives weak and unhealthy. So most of them sometimes fall sick in their respiration system. And that means they might unluckily get lung cancer if they take a lot of toxic pollution for a long time. So the researcher invented the odor eliminator by the electric field, "corona" for good health and protecting harmful disease for all people.

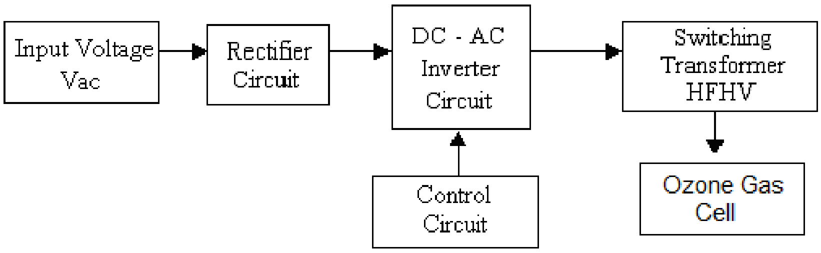

Figure 1 *Diagram block of odor eliminator.*

Materials and methods

A. The removal of the odor eliminator using pulse cool-corona electric field.

odor eliminator using pulse cool-corona electric field net has been adapted ionization and static electricity high voltage. This will make the air around the wire ionization rupture a charge by entering the high voltage direct current to the corona wire. This will cause the electric field intensity at the wire surface. When atoms or molecules of air into the air to break down by the principle that the atoms or molecules of the gas get enough energy to make it out to one electron. Atoms or molecules that have a positive charge are called the ionization process to separate the electrons from the particles of the gas. The process by which an electron is removed from a solid is called electron emission. In this way, electron is removed from the electrodes. A process, that is crucial will make the gas conductivity up. The energy from the electric field makes the air has got high intensity until it breaks and causing ozone. The ozone will eliminate odors and it can kill germs in the air as well.

The internal structure of the odor eliminator using pulse cool-corona electric field net. It consists of the following sections.

Part 1 : Pre - filter and blower.

Part 2 : High - voltage flyback converter circuit for generating pulse high voltage.

Part 3 : Cell electrode.

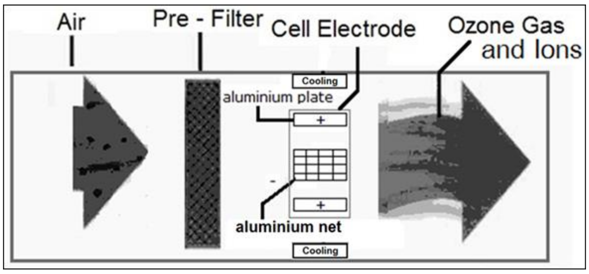

Figure 2 *The internal structure of the odor eliminator with electric field corona*

B. Thoery of generate ozone

Ozone gas is the gas occurred from 3 atoms of oxygen's gathing. Oxygen bond can be burst if the outside energy is fed to oxygen gas: O_2(g). The oxygen gas can be burst to be oxygen's free atoms. Then, they are again gathered to O_2 becoming to ozone gas O_3. The energy of ozone gas is less than oxygen gas O_2. In case of increasing energy to ozone gas O_3, only a little energy can cause O_3 to disintegrate. Thus, the system should not have too much heat inside the gap. For example, the heat from breakdown to generate ozone, the chemical energy interval is between 493.2 kJ/mol and 682.8 kJ/mol [1]. The unit can transform from mole to volume. Ideal gas has dotted model and has no strength to act each other. 1 mol of ideal gas is written in the relationship called gas equation, where n is amount of mole.Therefore, gas law is

$$PV = nRT \tag{1}$$

Real gas is found that gas molecules have the size and strength among molecules called Van der Walls. This is a kind of gas' quality. The approximate real gas equation is presented by Van der Walls in (2)

$$\left(p + \frac{a}{v^2}\right)(v - b) = RT \tag{2}$$

where V is the gas volume: m^3,

P is atmosphire pressure,

n is amount of moles,

R is gas constant,

P = 101.58 x 10^3 Pascal :Pa,

T = temperature :K,

$$R = 8314.3 \frac{Pa * m^3}{kmol * K}.$$

Define P = 101.5 kPa, T = 300 K , so V = 24.55 m^3/kmol
1 mol = 0.02455 m^3

Thus, 493.2 kJ/mol is 20089.61 kJ/m^3

and 682.8 kJ/mol is 27812.63 kJ/m^3

where 1J = 2.78 x 10^{-4} Wh

C. Plasma injector system for odor eliminator

Figure 3 shows the Plasma-injector system consists of a stainless steel cabinet with Plasma Reactors. Ambient air is radiated and, as a result, the oxygen and water vapour molecules are dissociated.

This transition is the first step in a process where eventually an extremely reactive gas is formed comprising a mixture of instable oxygen atoms, ions, radicals etc., with elevated electron energy levels. This gas, often called 'active oxygen' has the ability to execute a high speed oxidation process with odor components after injection in the polluted air. The odor molecules will lose the faculty of exciting man's sense of smell.

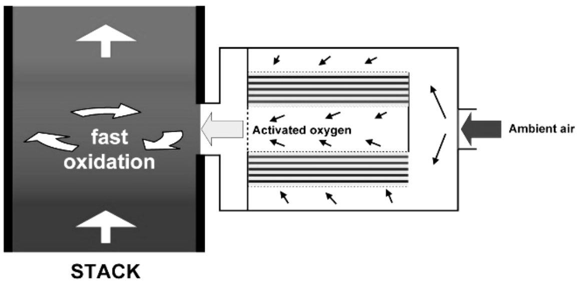

Figure 3 *Plasma injector [2]*

Oxidation:

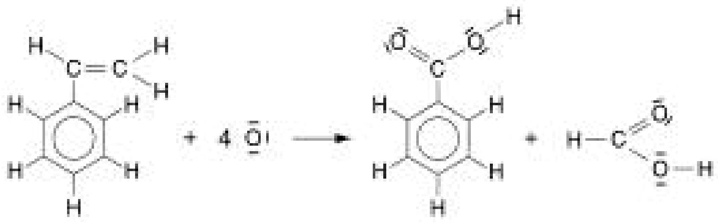

Figure 4 *Oxidation in the system of plasma injector*

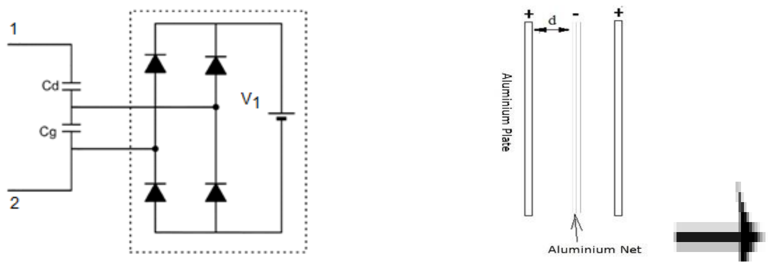

(a) (b)

***Figure* 5** *(a) Equipvalent circuit of ozone tube and (b) Cell electrode's structure [3]*

D. Volatile Organic Compounds (VOCs) or Hydrocarbon Compounds [4]

Definitions:

a) Volatile Organic Compounds (VOCs) – "VOCs are ground-water contaminants of concern because of very large environmental releases, human toxicity, and a tendency for some compounds to persist in and migrate with ground-water to drinking-water supply wells….In general, VOCs have high vapor pressures, low-to-medium water solubilities, and low molecular weights. Some VOCs may occur naturally in the environment, other compounds occur only as a result of manmade activities, and some compounds have both origins." – Zogorski and others, 2006.

b) Volatile Organic Compounds (VOCs) – "Volatile organic compounds released into the atmosphere by anthropogenic and natural emissions which are important because of their involvement in photochemical pollution." – Lincoln and others, 1998.

c) Volatile Organic Compounds (VOCs) – "Hydrocarbon compounds that have low boiling points, usually less than 100ºC, and therefore evaporate readily. Some are gases at room temperature. Propane, benzene, and other components of gasoline are all volatile organic compounds." – Art, 1993.

d) Volatile Organic Compounds (VOCs) – "VOCs are organic compounds that can be isolated from the water phase of a sample by purging the water sample with inert gas, such as helium, and, subsequently, analyzed by gas chromatography. Many VOCs are human-made chemicals that are used and produced in the manufacture of paints, adhesives, petroleum products, pharmaceuticals, and refrigerants. They often are compounds of fuels, solvents, hydraulic fluids, paint thinners, and dry-cleaning agents commonly used in urban settings. VOC contamination of drinking water supplies is a human-health concern because many are toxic and are known or suspected human carcinogens." – U.S. Geological Survey, 2005.

Results and discussion

A. Design and construction of cell electrode for generate ozone gas by calculation of high-voltage

Set the cell produce ozone gas. There is a distance between the aluminium plate with aluminium net (d) is equal to 1 centimeter and η^*equals 0.2 and therefore high voltage equal

$$V = E \times d \times \eta^{*}$$

At electric field E_i = 16.27 kV/cm ; V = 3.254 kV
At electric field E = 19.129 kV/cm **;** V = 3.825 kV

Thus, the voltage at the start of the corona is 3.254 kV to 3.825 kV at electric field 16.27 kV/cm to 19.129 kV/cm.

The cell electrode design is shown in Figure 6.

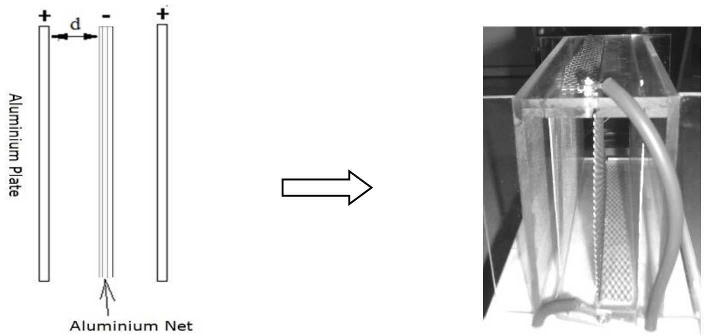

Figure 6 *The design: Making a thick plastic frame for holding the cell electrodes. The cell electrodes compose with two aluminum plates placed in parallel with the aluminium net that is inserted between the plates and then the amount of ozone will be produced when the eliminator begins working.*

B. The test of high voltage switching power supply and ozone gas analysis

The high voltage switching power supply as shown in Figure 7. Switching devices, Power MOSFET, are used in the flyback converter controlled by the PWM strategy from IC#SG3526. The switching frequency is 40 kHz. The energy supplied from the inverter can be transfered through a switching transformer to produce high voltage for the cell electrode.

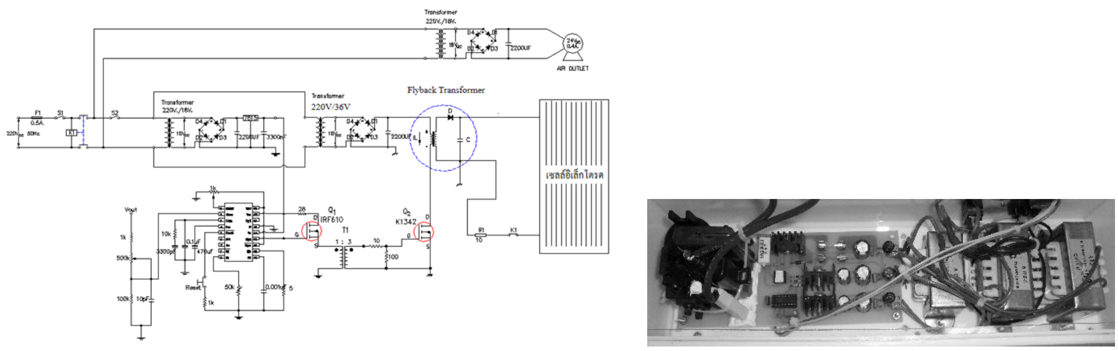

(a) (b)

Figure 7 *(a) The high voltage switching power supply and (b) The structure of high voltage switching power supply*

C. Ozone gas quantity and V_{GS} signal of IC#SG3526 output voltage at 3 kV of transformer.

From the experiment, the controlling circuit is set to have the switching frequency at 40 kHz, V_{out} is 3 kV and odor eliminator enables generate ozone gas of 5.83 ppm

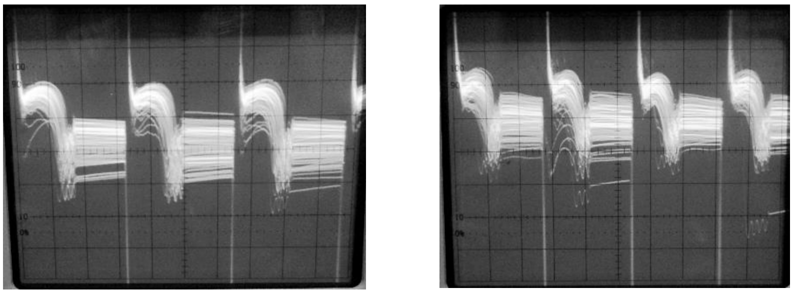

(a) (b)

Figure 8 *(a) Output high voltage of switching transformer at 2 kV at electric field intensity 10 kV/cm and (b) Output high voltage of switching transformer at 3 kV at electric field intensity 15 kV/cm.*

D. The relationship between high-voltage, ozone gas quantity and proved a foul odor. (By inhalation).

Table 1 *The relationship between high-voltage, ozone gas quantity and proved a foul odor. (By inhalation).*

V_{OUT} (kV)	Ozone gas quantity (ppm)	proved a foul odor (By inhalation)
1	3.96	×
2	4.43	×
3	5.83	✓

Parameter at table 1.

(✓ is Can get rid of the smell)

(× is Can't get rid of the smell)

E. The measurement of volatile organic compounds (VOCs) gas : (before and after of ozone gas injecting)

Table 2 *The measurement of volatile organic compounds (VOCs) gas : (before and after of ozone gas injecting) using frequency is 40 kHz, V_{OUT} is 3 kV and Ozone gas quantity of 5.83 ppm*

Sample (ozone injecting)	Volatile Organic Compounds (VOCs) Gas (ppm)
Before	531.9
After	3.7

F. The odor eliminator through the international standards of Electromagnetic Compatibility, EMC [CISPR 14-1 (CE, Click,PE), IEC61000-3-2 (HE), IEC 61000-3-3 (VF), CISPR 14-2 (CI, ESD, EFT, Surge, Vdip, PFM) is completed. Testing at the test room of electrical and electronic products testing center (PTEC), NSTDA, Thailand shown as Figure 9.

Figure 9 *Summary of testing EMC.*

G. The odor eliminator through tested analyze of the Power Consumption is completed. Testing at the test room of electrical and electronic products testing center (PTEC), NSTDA, Thailand.

H. Ozone gas quantity analysis Using Photometric O_3 Analyzer – Model 400E by ALS Laboratory group (Thailand) CO., LTD.

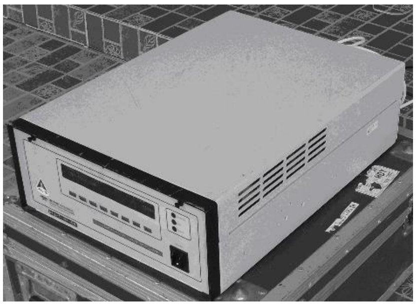

Figure 10 *Ozone gas quantity analyzer*

I. Special properties of the odor eliminator.

1. Eliminate unpleasant odors in the open and closed rooms such as a wardrobe and the rooms with or without air-conditioners.
2. Get rid of various kinds of smoke such as smoke from cigarette, incense etc. especially toxic gases.
3. Save money and preserve the environment because those used electrodes can be cleaned and put them back again and again.

J. Technique properties of the odor eliminator.

1. Ozone gas can decompose faster. So it isn't harmful to the users.
2. Pulse Corona Discharge technology.
3. Use with AC 220V/50Hz.
4. Output Voltage is 3 kV.
5. Use a power of 96 Watts.
6. Ozone gas quantity is 5.83 ppm.
7. Air Speed of 125 m/sec
8. Time to get rid of germs about 25 minutes.
9. The cost of odor eliminator is reasonable.

K. Utilization.

This odor eliminator can be used in many places such as in bedrooms, bathrooms, toilets and kitchens in houses, condominiums, foodshops and some herbal pharmacies as well. Besides it can be used in cars. The results after testing in those places the odors have been reduced and after several days they have been eliminated a lot. Then, there is none of the odors.

However the odor eliminator can get rid of the cat's urine odor in a room. And for the kitchen and the bathroom after the odor eliminator was used, the bad smell was reduced. Then the result is all of the odor has been got rid of.

How to test and measure the odor for the result

1. By men's smelling
2. By measuring the exposure of VOCs

Conclusions

The odor eliminator in this design and construction could be ozone gas by supplying the high voltage but not to strong to breakdown the generated ozone. From the test, high voltage of 3.25 kV was suitable to be used without breaking down the process. Ozone gas generating set was designed to use at 3 kV because it was the appropriate voltage to generate the maximum amount of ozone gas and provide not too much heat. Ozone gas did not quickly vanish, however the quantity of generated ozone can decrease odor (volatile organic compounds) (VOCs) or hydrocarbon gas from 531.9 ppm to 3.7 ppm and enables reduce global warming.

Then odor eliminator through the international standards of Electromagnetic Compatibility, EMC [CISPR 14-1 (CE, Click,PE), IEC61000-3-2 (HE), IEC 61000-3-3 (VF), CISPR 14-2 (CI,ESD, EFT, Surge, Vdip, PFM) and Tested analyze the Power Consumption are completed. Testing at the test room of electrical and electronic products testing center (PTEC), NSTDA, Thailand.

In the future, this technique could be utilized for other applications such as the air pollution treatment and kill bacterias.

Figure 11 *The structure of the odor eliminator with electrical field corona should be made of plaswood for it must be strong for it can prevent the leakage of electricity as well. Then all of electronic equipments are installed. After that the odor eliminator is ready to eliminate all the toxic odor and smoke.*

Material used in the research invention and sources.

1. A plaswood frame.
2. Two aluminum plates.
3. Aluminium net.
4. A blower.
5. Electronic equipments.

(Note : Cool-Corona *means reducing the heat while the corona discharge process in order to increase the efficiency of ozone production based on the adjustment of electric energy to be appropriate.*)

Acknowledgements

This research innovation was funded activities to promote and support research of the National Research Council of Thailand (NRCT) 2016.

References

[1] S.Ketkaew, “The study of ozone gas generating technique using high frequency, high voltage dc switching power supply of high ripple voltage”(in Thai), J. KMITL. 22, 1 (2005).

[2] How Cold Plasma Injection Technology Works, http://www.uniqair.com/, 5 March 2016.

[3] J. Alonso, J. Cardesín, E. L. Corominas, M. Rico-Secades and J. García, “Low-Power High-Voltage High-Frequency Power Supply for Ozone Generation”, IEEE Trans. Ind. Appl. 40, 414 (2004).

[4] Volatile Organic Compounds in Your Home, http://www.health.state.mn.us/divs/eh/indoorair/voc, 2 January 2016.